# GROUND-BASED HIGH-RESOLUTION INFRARED AND SUBMILLIMETER SEARCHES FOR THE RELEASE OF VOLCANIC GASES ON MARS.

**A. SJ. Khayat**[1,2], **G.L. Villanueva**[1], **M.J. Mumma**[1], **A.T. Tokunaga**[3], *(alain.khayat@nasa.gov)* [1]*NASA Goddard Space Flight Center;* [2]*University of Maryland, College Park, USA;* [3] *Institute for Astronomy, University of Hawaii, Honolulu, Hawaii, USA*.

## Introduction

Recent volcanic activity has long been considered a distinct possibility that would place major constraints on the evolution of Mars' interior. Volcanic activity would result in the outgassing of sulfur-bearing species. As part of our multi-band search for active release of volcanic gases on Mars, we looked for carbonyl sulfide (OCS) at its combination band ($\nu_1$+$\nu_3$) at 3.42 $\mu$m (2924 cm$^{-1}$), and sulfur dioxide ($SO_2$) at 346.652 GHz, in two successive Mars years during its late Northern spring and mid Northern summer seasons ($L_s$= 43°-144°). The targeted volcanic districts, Tharsis and Syrtis Major, were observed during two intervals, 15 Dec. 2011 to 6 Jan. 2012 in the first year, and 23 May 2014 to 12 June 2014 in the second year using the NASA Infrared Telescope Facility (IRTF), and the James Clerk Maxwell Telescope (JCMT) atop Maunakea, Hawaii. We report our results and discuss their implications for current volcanic outgassing on the red planet.

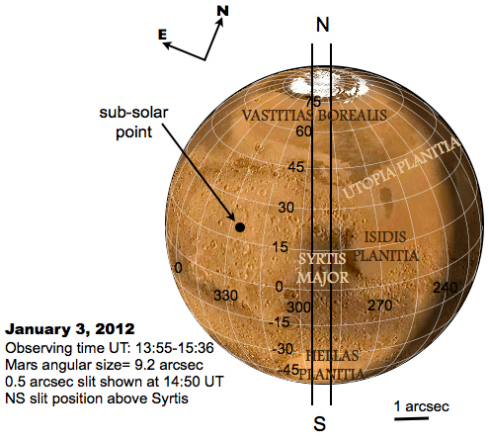


Figure 1: The panel shows CSHELL's slit covering the N-S central meridian of Mars on January 3, 2012. The two parallel lines represent the entrance slit that is shown to scale, with a 0.5 arcsec width. The perpendicular arrows on the top left of each panel represent the directions of the celestial North and East.

## Observations

The infrared observations were carried out using CSHELL [19, 7] a high-resolution infrared spectrometer (resolving power of R = $\nu/\Delta\nu \sim$ 43,000) at the 3 m IRTF. We positioned CSHELL's entrance slit (0.5 × 30 arcsec$^2$) on the North-South central meridian of Mars, and took spectra while the planet rotated under the slit, therefore scanning the targeted volcanic regions on Mars under the sub-Earth point (Figure 1). We nodded the telescope in two Mars positions along the slit (labeled "A" and "B"), separated by 15 arcsec, and took a series of 4 exposures (ABBA), with 1 minute on-source integration time per position. The quantity (A1-B1-B2+A2) cancels the telluric and telescope emissions to first order about the mean airmass. After forming this sum, the residuals at the A and B positions in the spectral frame are the spectra of Mars (emission and absorption) multiplied by Earth's atmospheric transmittance.

The submillimeter observations were made using the single sideband high resolution Heterodyne Array Receiver Program (HARP) [1], located in the right Nasmyth focus of the 15 m single dish antenna of the JCMT, at a resolving power R $\sim$ 580,000. At the back end of the receiver HARP, the digital autocorrelation spectrometer ACSIS was used at the band-width and channel spacing mode 1000 MHz × 2048. The targeted volcanic area, Tharsis, was observed at the respective sub-Earth point. The angular size of Mars was 12.5 arcsec in the middle of the run between 23, 24 and 25 May 2014, and the average telluric optical depth at 225 GHz, $\tau_{225\mathrm{GHz}}$, a proxy for the amount of water vapor and extinction in Earth's atmosphere, ranged between 0.10 and 0.13. The beam of the JCMT at 346.5 GHz has a FWHM of 14.5 arcsec. The chopping between Mars and the sky was conducted at 60 arcsec from the planet.

## Data processing and results

Infrared data: On every night, we obtained flat and dark frames at the OCS frequency setting for data calibration purposes. The data were processed using a data reduction and analysis pipeline, coded in IDL and based on algorithms specifically developed for CSHELL observations [22, 13, 21, 23]. In order to correct for the tilt of the spectral lines, we relied on a Line-By-Line Radiative Transfer Model (LBLRTM) [2] in synthesizing Earth's atmospheric transmittance spectra. The modeled

telluric spectra were compared row-by-row and line-by-line to the observed telluric absorption in order to adjust for the tilt of the spectral lines. The same techniques for straightening and and linearizing the spectra are detailed in [22, 23]. For some settings, solar Fraunhofer lines, originating from the solar reflected radiation, appear in the flux received from Mars, and this permits estimation of the ratio of Mars thermal emission to the reflected sunlight. The thermal emission is subjected to a one way airmass between Mars' surface and the observer, whereas the solar radiation goes through a two-way airmass (Sun-Mars'-surface and Mars'-surface-observer). Measuring the diminished equivalent width of the Fraunhofer lines in the emergent flux from Mars indicates the contribution of the reflected solar radiation to the total radiation received from the planet [15]. This contribution is crucial in modeling the spectral lines from the martian atmosphere. At 2924 $\mathrm{cm}^{-1}$, the equivalent width of the solar lines shows that the emergent intensity from Mars is mostly solar radiation, i.e. Mars is seen predominantly in reflected sunlight. Observing Mars through the Earth's atmosphere introduces spectral features in the martian spectrum. To correct for telluric absorption, we applied the technique developed in [21] by using the LBRTM to synthesize the Earth's atmospheric transmittance spectra.

In order to increase the signal-to-noise ratio, we co-added the residual spectra (difference of the observed minus the model spectrum) along the slit in the spatial direction. We then sliced and co-added OCS lines within $\pm$ 7 sampling elements around line centers. The line strength at the first scale height in the martian atmosphere is used as the weighting factor, and the spectroscopic parameters for the OCS transitions that were extracted from the HITRAN 2012 database [18, 17]. At each night, we co-added the residual spectra at the appropriate OCS transitions where there are no systematic features in the residuals, leading to a combined line spectrum with the highest SNR. This did not reveal any OCS absorption feature. In the final step, we combined the data over 4 key dimensions: latitude, longitude, time between 2011 and 2014, and frequency. We then synthesized a Gaussian OCS line with FWHM equal to the CSHELL spectral resolution, and extracted the upper limit on the mixing ratio. The resulting spectrum is shown in Figure 2. Table 1 presents the upper limits at $2\sigma$ on the OCS abundance.

Submillimeter data: We applied the same techniques we developed to analyze the previous data from our Mars 2011 and 2012 observations with the Caltech Submillimeter Observatory (see section 3 in [8]). To model the spectral lines of $SO_2$, we rely on the measured physical conditions on Mars, which include the surface temperature, pressure, and the thermal structure in the martian atmosphere. On May 25, 2014, we estimated the a-priori disk-averaged brightness temperature of Mars, $T_b$ = 221.16 K, using the surface temperature from the

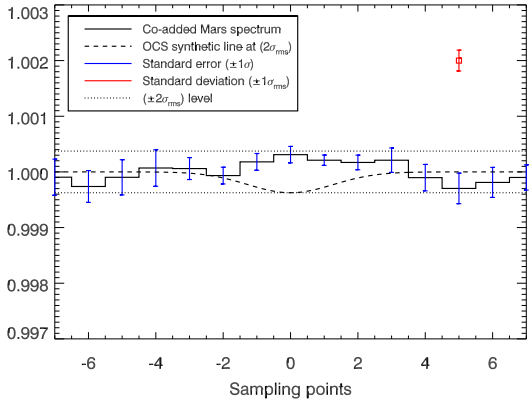


Figure 2: After co-adding the line spectra between December 15, 2011 and June 12, 2014, we achieved a SNR derived from the standard deviation in the spectrum of 5,350. The blue error bars are the standard errors for each pixel, the red error bar is $\pm 1\sigma_{rms}$ over the spectrum (solid black), and the dashed black line is the synthetic OCS line at $2\sigma_{rms}$ level.

Mars Climate Database (MCD) [11, 6], and the emissivity of the martian soil. We divided the disk of the planet into 36$\times$36 equally-sized bins, and extracted the temperature profiles from the MCD at each bin at the time of the observation. Using these a-priori profiles and the surface temperature, we modeled the observed atmospheric $^{12}$CO (3-2) spectral line (rest frequency at 345.796 GHz). We applied the Levenberg-Marquardt retrieval process to modify the temperature profiles and the surface temperature, in order to minimize the residuals between the model and the data. This spectral inversion method leads to 36$\times$36 fitted profiles for Mars, and the profile which gives the best fit between all the other fitted-profiles, was subsequently used for the three consecutive nights of May 23, 24 and 25. We used a radiative transfer model in [8] to synthesize the spectral line, with the appropriate line shape parameters for $SO_2$ in the Mars' $CO_2$ dominant atmosphere. The spectral lines are modeled at a spectral resolution of $\sim 5\times10^{-3}$ MHz, then convolved with a boxcar kernel of 0.59 MHz width, the spectral resolution of the ACSIS spectrometer. We later interpolated these values with the channel spacing of 0.49 MHz in order to compare our synthetic line shapes with the combined measured spectrum. No spectral absorption of $SO_2$ on any of the dates was found. We co-added the 3 nights, and achieved an rms of 0.045% on the normalized continuum level. The Mars and the synthetic $SO_2$ spectra at $2\sigma$ are shown in Figure 3, and the corresponding abundance limits are listed in Table 1.

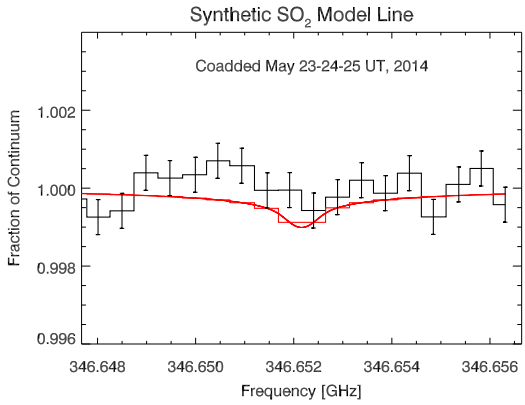


Figure 3: The spectrum of the co-added data for May 23, 24 and 25 UT, 2014. The black solid line shows the spectrum of $SO_2$. The spectra are normalized to the continuum of Mars and shifted to the rest frequency. The solid red lines show the expected absorption at $2\sigma$.

Table 1: Abundance limits ($2\sigma$) for OCS and $SO_2$ obtained in this work compared to previous work.

| Date (UT) | Volcanic Region | Number of transitions used | Upper limit at $2\sigma$ (ppbv) | Previous (ppbv) |
|---|---|---|---|---|
| Molecule: OCS | | | | |
| 15 December 2011 | Tharsis | 4 | <4.3 | |
| 18 December 2011 | Tharsis | 4 | <4.4 | |
| 3 January 2012 | Syrtis Major | 4 | <3.8 | |
| 5 January 2012 | Syrtis Major | 4 | <3.8 | |
| 6 January 2012 | Syrtis Major | 4 | <4.2 | |
| 30 May 2014 | Tharsis | 5 | <3.5 | |
| 12 June 2014 | Syrtis Major | 4 | <2.4 | |
| Co-added over | | | <**1.8** | <10 (in the IR, [12] |
| all nights | | | <**1.8** | <70 (in the mm, [5] |
| Molecule: $SO_2$ | | | | |
| 23 May 2014 | Tharsis | 1 | <5.1 | |
| 24 May 2014 | Tharsis | 1 | <5.2 | |
| 25 May 2014 | Tharsis | 1 | <6.4 | |
| Co-added over | | | <**3.1** | <0.3 (in the IR) |
| all nights | | | | [10] and |
| | | | | [4] |
| | | | <**3.1** | <1.1 (in the submm) |
| | | | | [8] |

## Conclusion

When spread uniformly across the disk of Mars, our retrieved upper limit on the mixing ratio of 3.1 ppbv for $SO_2$ corresponds to a mass of 114 kilotons. This limit, combined with a lifetime of 2 years for $SO_2$ [14, 9], yields an outgassing rate of $SO_2$ of less than 156 tons/day between 23 and 25 May 2014, if the release is steady. As a comparison with a terrestrial analog to the Tharsis volcanoes, Kilauea volcano in Hawaii releases $SO_2$ on an average rate of 1650 tons/day [3].

Our upper limit of 1.8 ppbv on OCS establishes constraints on the chemical reaction forming OCS from $SO_2$ and CO, whether in terms of the equilibrium temperature, the low amounts of $SO_2$, or both. Combined with that of OCS, the upper limit on $SO_2$ establishes limits on the release of volcanic gases at the present time on Mars.

Great advances on this matter will be pursued with ExoMars/Trace Gas Orbiter [20]. Future prospects for detecting OCS and $SO_2$ involving ground-based facilities include iSHELL, a high-resolution immersion grating spectrograph, operating between 1.15 to 5.4 $\mu$m. iSHELL is the next generation high-resolution spectrograph on the IRTF. The instrument is a cross-dispersed spectrograph, providing a 20-100 times larger simultaneous wavelength coverage as compared to the single order spectrograph CSHELL [16]. iSHELL offers a 70,000 spectral resolving power that allows distinguishing weaker lines in the martian atmosphere, and separating them from their telluric counterparts. The instrument provides the whole OCS ($\nu_1$+$\nu_3$) band to be sampled simultaneously, thus improving the detection limit by combining data from multiple lines.

## Acknowledgments

We gratefully acknowledge the support from the NASA Planetary Astronomy Program under Cooperative Agreement NNX08AE38A, NASA contract NNH14CK55B, RTOP 344-32-07 and NASA's Astrobiology Program (RTOP 344-53-51) that supported M.J.M., and G.L.V.

## References

[1] J. V. Buckle, R. E. Hills, H. Smith, W. R. F. Dent, G. Bell, E. I. Curtis, R. Dace, H. Gibson, S. F. Graves, J. Leech, J. S. Richer, R. Williamson, S. Withington, G. Yassin, R. Bennett, P. Hastings, I. Laidlaw, J. F. Lightfoot, T. Burgess, P. E. Dewdney, G. Hovey, A. G. Willis, R. Redman, B. Wooff, D. S. Berry, B. Cavanagh, G. R. Davis, J. Dempsey, P. Friberg, T. Jenness, R. Kackley, N. P. Rees, R. Tilanus, C. Walther, W. Zwart, T. M. Klapwijk, M. Kroug, and T. Zijlstra. *Monthly Notices of the Royal Astronomical Society*, 399:1026–1043, Oct. 2009.

[2] S. A. Clough, M. W. Shephard, E. J. Mlawer, J. S. Delamere, M. J. Iacono, K. Cady-Pereira, S. Boukabara, and P. D. Brown. *J. Quant. Spectrosc. Radiat. Trans.*, 91(2):233–244, Mar. 2005.

[3] T. Elias and A. Sutton. *U.S. Geological Survey Open-File Report 2012-1107, Available online at http://pubs.usgs.gov/of/2012/1107/*, pages 1–25, 2012.

[4] T. Encrenaz, T. K. Greathouse, M. J. Richter, J. H. Lacy, T. Fouchet, B. Bézard, F. Lefèvre, F. Forget, and S. K. Atreya. *Astron. & Astrophys.*, 530:A37, June 2011.

[5] T. Encrenaz, E. Lellouch, J. Rosenqvist, P. Drossart, M. Combes, F. Billebaud, I. de Pater, S. Gulkis, J. P. Maillard, and G. Paubert. *Ann. Geophys.*, 9:797–803, Dec. 1991.

[6] F. Forget, F. Hourdin, R. Fournier, C. Hourdin, O. Talagrand, M. Collins, S. R. Lewis, P. L. Read, and J.-P. Huot. *J. Geophys. Res.*, 104:24155–24176, Oct. 1999.

[7] T. P. Greene, A. T. Tokunaga, D. W. Toomey, and J. B. Carr. In A. M. Fowler, editor, *Infrared Detectors and Instrumentation*, volume 1946 of *Society of Photo-Optical Instrumentation Engineers (SPIE) Conference Series*, pages 313–324, Oct. 1993.

[8] A. S. Khayat, G. L. Villanueva, M. J. Mumma, and A. T. Tokunaga. *Icarus*, 253:130–141, June 2015.

[9] V. A. Krasnopolsky. *J. Geophys. Res.*, 100:3263–3276, Feb. 1995.

[10] V. A. Krasnopolsky. *Icarus*, 217:144–152, Jan. 2012.

[11] S. R. Lewis, M. Collins, P. L. Read, F. Forget, F. Hourdin, R. Fournier, C. Hourdin, O. Talagrand, and J.-P. Huot. *J. Geophys. Res.*, 104:24177–24194, Oct. 1999.

[12] W. C. Maguire. *Icarus*, 32:85–97, Sept. 1977.

[13] M. J. Mumma, G. L. Villanueva, R. E. Novak, T. Hewagama, B. P. Bonev, M. A. DiSanti, A. M. Mandell, and M. D. Smith. *Science*, 323:1041–1045, Feb. 2009.

[14] H. Nair, M. Allen, A. D. Anbar, Y. L. Yung, and R. T. Clancy. *Icarus*, 111:124–150, Sept. 1994.

[15] R. E. Novak, M. J. Mumma, M. A. DiSanti, N. D. Russo, and K. Magee-Sauer. *Icarus*, 158:14–23, July 2002.

[16] J. Rayner, T. Bond, M. Bonnet, D. Jaffe, G. Muller, and A. Tokunaga. In *Society of Photo-Optical Instrumentation Engineers (SPIE) Conference Series*, volume 8446 of *Society of Photo-Optical Instrumentation Engineers (SPIE) Conference Series*, page 2, Sept. 2012.

[17] L. Régalia-Jarlot, A. Hamdouni, X. Thomas, P. V. der Heyden, and A. Barbe. *J. Quant. Spectrosc. Radiat. Trans.*, 74:455–470, 2002.

[18] L. Rothman, I. Gordon, Y. Babikov, A. Barbe, D. C. Benner, P. Bernath, M. Birk, L. Bizzocchi, V. Boudon, L. Brown, A. Campargue, K. Chance, E. Cohen, L. Coudert, V. Devi, B. Drouin, A. Fayt, J.-M. Flaud, R. Gamache, J. Harrison, J.-M. Hartmann, C. Hill, J. Hodges, D. Jacquemart, A. Jolly, J. Lamouroux, R. L. Roy, G. Li, D. Long, O. Lyulin, C. Mackie, S. Massie, S. Mikhailenko, H. MÃ…ller, O. Naumenko, A. Nikitin, J. Orphal, V. Perevalov, A. Perrin, E. Polovtseva, C. Richard, M. Smith, E. Starikova, K. Sung, S. Tashkun, J. Tennyson, G. Toon, V. Tyuterev, and G. Wagner. *J. Quant. Spectrosc. Radiat. Trans.*, 130:4 – 50, 2013. HITRAN2012 special issue.

[19] A. T. Tokunaga, D. W. Toomey, J. Carr, D. N. B. Hall, and H. W. Epps. In D. L. Crawford, editor, *Instrumentation in Astronomy VII*, volume 1235 of *Society of Photo-Optical Instrumentation Engineers (SPIE) Conference Series*, pages 131–143, July 1990.

[20] A. C. Vandaele, E. Neefs, R. Drummond, I. R. Thomas, F. Daerden, J.-J. Lopez-Moreno, J. Rodriguez, M. R. Patel, G. Bellucci, M. Allen, F. Altieri, D. Bolsée, T. Clancy, S. Delanoye, C. Depiesse, E. Cloutis, A. Fedorova, V. Formisano, B. Funke, D. Fussen, A. Geminale, J.-C. Gérard, M. Giuranna, N. Ignatiev, J. Kaminski, O. Karatekin, F. Lefèvre, M. López-Puertas, M. López-Valverde, A. Mahieux, J. McConnell, M. Mumma, L. Neary, E. Renotte, B. Ristic, S. Robert, M. Smith, S. Trokhimovsky, J. Vander Auwera, G. Villanueva, J. Whiteway, V. Wilquet, and M. Wolff. *Planet. Space Sci.*, 119:233–249, Dec. 2015.

[21] G. L. Villanueva, M. J. Mumma, and K. Magee-Sauer. *J. Geophys. Res.*, 116(E8):E08012, Aug. 2011.

[22] G. L. Villanueva, M. J. Mumma, R. E. Novak, and T. Hewagama. *Icarus*, 195:34–44, May 2008.

[23] G. L. Villanueva, M. J. Mumma, R. E. Novak, Y. L. Radeva, H. U. Käufl, A. Smette, A. Tokunaga, A. Khayat, T. Encrenaz, and P. Hartogh. *Icarus*, 223(1):11–27, Mar. 2013.